electronic reprint

Journal of
Applied Crystallography
ISSN 0021-8898

Small-angle neutron scattering investigation of deuteride (hydride) precipitation and decomposition in single-crystal Pd

W.C. Chen, B.J. Heuser and J.S. King

Small-angle neutron scattering investigation of deuteride (hydride) precipitation and decomposition in single-crystal Pd

W.C. Chen,[a] Brent J. Heuser[a]* and John S. King[b]

[a]*University of Illinois, Department of Nuclear, Plasma and Radiological Engineering, Urbana, IL 61801, USA, and* [b]*University of Michigan, Department of Nuclear Engineering and Radiological Sciences, Ann Arbor, MI 48109, USA.* *E-mail: bheuser@uiuc.edu*

Small-angle neutron scattering (SANS) measurements of deuteride formation and decomposition in single crystal Pd have been performed. The purpose of this work was to determine and compare the particle morphology during deuteride precipitation and reversion, with the overall goal of developing a model for the pressure hysteresis known to exist in the Pd-H system. Anisotropic Porod scattering at low Q was observed as the samples were driven well into the two-phase region from either solid solution (the $\alpha \rightarrow \alpha'$ transformation) or from 100% α' (the $\alpha' \rightarrow \alpha$ reversion). This scattering is attributed to the formation of large, presumably semi-coherent or completely incoherent, tens-of-microns thick plates on well-defined habit planes. The orientation and dispersion of these larger plates was different for deuteride formation and decomposition: a very coarse dispersion on the $\{110\}_{\alpha}$ habit plane developed during deuteride formation, while a much finer dispersion on the $\{100\}_{\alpha'}$ habit plane occurred during deuteride reversion from the 100% deuteride phase. The latter orientation is consistent with the system selecting the habit plane orthogonal to the softest host direction to minimize the elastic accommodation energy of the precipitates. We suspect the $\{110\}_{\alpha'}$ habit plane observed during deuteride formation is related to large over-pressure loading conditions. An isotropic SANS response from plates with thicknesses of 20 to 30 Å was also observed during deuteride formation and reversion. These plates are thought to act as (coherent) precursors to the large plate formation.

1. Introduction

The properties of hydrogen and hydrogen isotopes in Pd have been of studied for several decades and are well characterized under a variety of conditions. One particular property, the unequal isothermal pressure plateau values during gas-phase absorption and desorption (the pressure hysteresis) is also well characterized, but a conclusive explanation still eludes the scientific community. Observation of the pressure hysteresis in the Pd-H system dates to the year 1911 (Lewis, 1967). The generally accepted explanation attributes the pressure hysteresis to the irreversible formation of dislocations at incoherent hydride-host matrix interfaces during precipitation and dissolution (Flanagan *et al*., 1980; Flanagan and Clewley, 1982). This explanation is consistent both with the known transformation volume misfit between the solid solution α phase and the hydride α' phase (approximately 11%) and with the lattice damage observed upon hydride formation and dissolution (Lynch *et al*., 1977; Jamieson *et al.*, 1976).

More recently, an explanation of the hysteresis phenomenon that is applicable to metal-hydrogen systems has been advanced by Schwarz and Khachaturyan (1995). These authors propose that isothermal pressure hystereses common in metal-hydrogen systems are a direct consequence of coherent elastic free energy. The existence of this free energy invalidates the Gibbs phase rule governing incoherent phase separation and prohibits the nucleation of incoherent particles (Cahn and Larché, 1984). Schwarz and Khachaturyan extend these arguments (for an elastically isotropic host matrix) and demonstrate, at least theoretically, that the pressure hysteresis is the result of a lack of two-phase equilibrium in a coherent, open system. This is clearly inconsistent with the incoherent nature of the phase transformation thought to exist in the Pd-H system. A key assumption in the Schwarz-Khachaturyan hypothesis is the starting point--an elastically isotropic host matrix. Eshelby (1957) has shown that the elastic strain energy of a coherent particle embedded in such a matrix is independent of the particle shape. Schwarz and Khachaturyan use this fact to derive an express for the system free energy that is independent of hydride phase particle shape and orientation relative to the host lattice. A minimization of this free energy with respect to internal thermodynamic variables leads to the their hypothesis.

Palladium is, like most metals, elastically anisotropic (anisotropy ratio of 2.81 at 300 K; Hsu and Leisure, 1979). Elastic anisotropy is expected to influence the hydride formation and dissolution process (Porter and Easterling, 1992). Characterization of the hydride morphology in Pd is, therefore, useful, especially since this information is lacking for the Pd-H system. The SANS technique is sensitive to the formation and dissolution of the deuteride phase and can yield particle morphological information with the use of single crystal material.

2. Experimental

The experimental procedures used followed those specified in a previous publication (Heuser *et al.*, 1999) and are only briefly outlined here. Well-annealed, single crystal Pd samples were prepared from a 99.999% pure single crystal Pd ingot grown by Metal Crystals and Oxides of Cambridge, England. The cylindrical ingot was grown by the Czochralski method with a [110] axis, 10 cm in length and approximately 1.0 cm in diameter. Samples were cut from the as-grown ingot using a low speed diamond saw and mechanically polished to remove surface irregularities. 0.03 μ levitated alumina was used in the final polishing step. The crystallographic orientation of the samples were determined by x-ray diffraction.

Small-angle neutron scattering (SANS) data from deuteride α' dissolution during *in situ* gas-phase desorption at 353 K will be presented below. These data will be compared with previous SANS data taken during deuteride formation during room temperature gas-phase absorption (Heuser *et al.*, 1999). In addition to the different measurement temperatures, other differences in the physical properties of the two sample types (absorption and desorption) deserve discussion. First, the

absorption samples consisted of two identical wafers, each approximately 1 cm diameter and 0.16 cm thick (1.5 g. in weight). This was done to facilitate deuterium loading. The desorption sample consisted of a single wafer of approximately equal dimensions as a single absorption wafer. Finally, the desorption sample had undergone complete $\alpha \rightarrow \alpha'$ conversion prior to SANS investigation. Thus, the starting point of the characterization of this sample was the 100% α' phase. Ultra high vacuum stainless steel gas cells were used for the SANS measurements. The cells were equipped with two sapphire windows to reduce empty-cell neutron scattering. Deuterium loading was accomplished by exposure to deuterium gas. Deuterium concentrations were calculated from the measured pressure changes (the volumetric technique) and are accurate to within 10% for concentrations below approximately 0.1 [D]/[Pd] and to within a five percent error at higher concentrations.

The SANS measurements were performed at the National Institute of Standards and Technology Center for Neutron Research using the NG3 instrument. The two instrument configurations, an intermediate-Q configuration ($0.007 \leq Q \leq 0.1$ Å^{-1}, where Q is given by $Q=(4\pi/\lambda) \sin \theta$, λ is the neutron wavelength and θ is half the scattering angle) and a high-Q configuration ($0.03 \leq Q \leq 0.4$ Å^{-1}), used for the present work were identical to that employed previously (Heuser *et al.*, 1999). The neutron wavelength for both NIST measurements was 6.0 ± 0.9 Å (± FWHM). Absolute cross section calibration was performed in the high-Q configuration using the incoherent scattering from 0.1 cm of water. The low-Q data were then scaled to the high-Q cross sections over a common data range of approximately $0.04 \leq Q \leq 0.08$ Å^{-1}.

3. Results and discussion

The 300 K and 353 K solubility isothermal measurements performed using the single crystal material are shown in Fig. 1. The location of SANS measurements performed along each isotherm are also identified on this figure. The radial-averaged net SANS response, given by the absolute macroscopic, differential cross section $d\Sigma/d\Omega$, of early α' phase formation in the host α matrix (at 300 K) and of early α formation in the α' matrix (at 353 K) are compared in Fig. 2. These data were roughly isotropic and follow, after incoherent background subtraction, the single particle form factor for a plate given by (Porod, 1982),

$$\frac{d\Sigma}{d\Omega}(Q) = 2\pi \, f \, T \frac{\Delta\rho^2}{Q^2} \exp\left(-Q^2T^2/12\right) , \qquad (1)$$

where f is the volume fraction of deuteride particles resulting in the Q^{-2} response, $\Delta\rho$ is the scattering length density contrast between the deuteride phase and the Pd matrix ($\Delta\rho = 2.1 \times 10^{10}$ cm^{-2}), and T is the plate thickness. The thickness T is obtained from fitting the highest Q portion of the data where the exponential modifier in equation 1 strongly affects the scattering response. A thickness of 20 to 30 Å is characteristic of both α' formation in α and α formation in α'. The observation of an isotropic distribution of small plates indicates the initial phase nucleation process is coherent without a preferred habit plane.

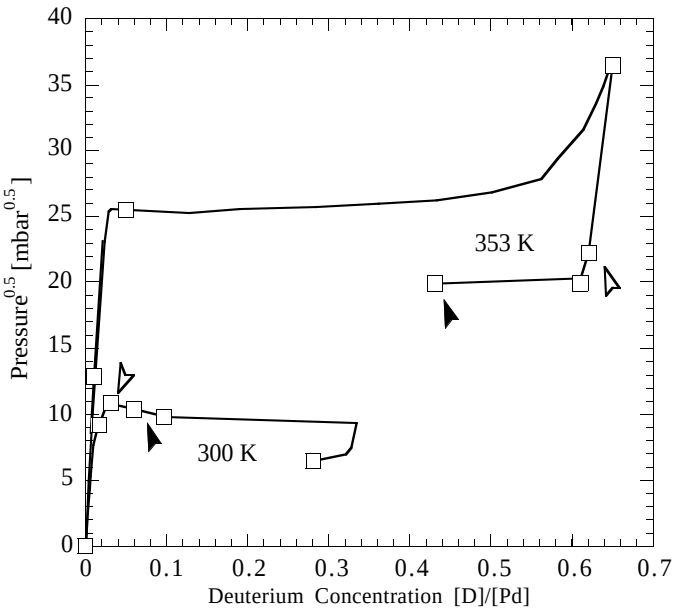

Figure 1
Measured Pd-D isotherms for single crystal material. The full 300 K isotherm was not recorded. Open boxes indicate locations of SANS measurements along isotherms. Open arrows show the concentration of the SANS measurements presented in Fig. 2, while closed arrows show the concentration of the SANS measurements given in Fig. 3.

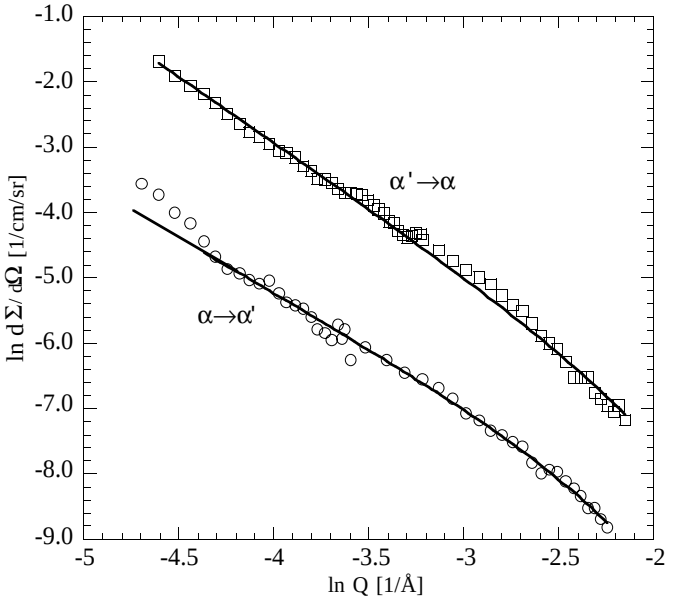

Figure 2
Net SANS response from deuteride formation (open circles) and reversion (open boxes) early in the respective phase transformation processes. The net response is defined either as the difference between the with-deuterium measurement and the zero-concentration measurement (absorption data) or the difference between the reduced deuterium concentration measurement and the 100% α' measurement (desorption data). Two Q range configurations are spliced together for each data set. Solid lines are best fits of equation 1 to the net data. The roll-over at highest Q in each data set is the result of the small but finite plate thickness. Fit of this roll-over with the Guinier-type exponential term in equation 1 yields the characteristic plate thickness.

Table 1
Fitting parameters from measured SANS cross sections.

Sample [D]/[Pd]	Q^{-2} amplitude (10^{-5} cm^{-1}Å^{-2}sr^{-1})	f (10^{-5})	T (Å)	Q^{-4} amplitude (10^{-9} cm^{-1}Å^{-4}sr^{-1})	S/V (cm^{-1})
Fig. 2 data					
0.031	0.24 ± 0.03	3	25	0.08 ± 0.02	1.2
0.62	1.86 ± 0.03	27	20	—	—
Fig. 3 data					
0.060	0.73 ± 0.02	8	27	0.18 ± 0.02	2.6
0.43	6.83 ± 0.06	74	27	37.3 ± 0.5	550

Two other aspects of the data in Fig. 2 deserve discussion. First, the Q^{-2} scattering amplitude is much larger for the $\alpha' \rightarrow \alpha$ data. For equal plate thickness, this amplitude is proportional to the volume fraction of the plate-like particles. The volume fractions and plate thicknesses obtained from the application of equation 1 are listed in Table 1. The second aspect of Fig. 2 is that the desorption measurement point is actually above the pressure plateau. That precipitation is observed *before* the plateau is surprising. This suggests dissolution of the α' phase begins prior to the desorption plateau, at least on a microscopic scale characterized by the formation of very small plates. This would contradict the phase rule (exluding internal stress as a degree of freedom), however. Further SANS measurements are planned to investigate the initial dissolution process more completely.

The radial-averaged, net SANS responses at deuterium concentrations further into the miscibility gap from solid solution and from 100% α' are compared in Fig. 3. Notice the Q^{-2} scattering response still characterizes the $\alpha \rightarrow \alpha'$ transformation process over most of the measured Q range. At lowest Q, however, the measured response deviates upward from the Q^{-2} power law. The excess scattering is attributed to Porod scattering given by (Roth, 1977),

$$\frac{d\Sigma}{d\Omega}(Q) = \frac{4\pi \Delta\rho^2}{Q^4}\frac{S}{V} \quad , \qquad (2)$$

where S/V is the orientation-averaged surface-to-volume ratio of the scattering objects. We make this assertion even though the excess signal is weak for the absorption data. It is based on the visual observation of large, 100 μ thick plate-like particles with an orientation that matched the observed scattering anisotropy (scattering anisotropy reproduced below; see also Heuser *et al*., 1999 and Heuser *et al*., 2000). As with the Fig. 2 data, the Q^{-2} response from the dissolution sample ($\alpha' \rightarrow \alpha$ transformation) is much stronger (see Table 1) in Fig. 3. In addition, the deviation from the Q^{-2} power law at low Q is much stronger and clearly Porod. Again, this is the asymptotic response of large objects, identified as plates based on the nature of the scattering anisotropy discussed below.

The S/V ratio determined from the application of equation 2 to the excess low Q scattering in Fig. 3 is listed in Table 1. (Note that excess scattering can also be resolved in the absorption data presented in Fig. 2. The Porod S/V ratio for this excess scattering is listed in Table 1 as well.) The two SANS measurement concentrations in Fig. 3 are well removed from the respective phase boundaries. The volume fractions of the precipitating phase given by the lever rule are different by a factor of four; 8% and 30% for α' formation in α and α formation in α', respectively. The volume fraction, f, of the small plates resulting in the Q^{-2} scattering behavior given in Table 1 is remains small compared to the total volume fraction of the precipitating phase. The vast majority of the second phase is in the form of the large, oriented plates responsible for the Porod scattering at low Q. The S/V ratios in Table 1 indicates the dispersion of α in α' is much finer than of α' in α.

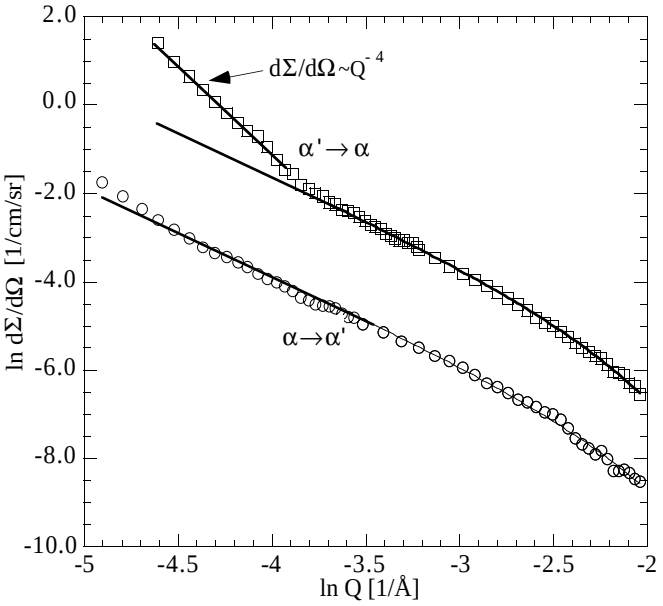

Figure 3
Net SANS response from deuteride formation (open circles) and reversion (open boxes) later in the respective phase transformation processes. Two Q range configurations are spliced together for each data set. Solid lines are best fits of equation 1 to the net data. Strong excess Porod scattering at lowest Q is evident for the desorption data.

Unlike the isotropic Q^{-2} scattering, the Porod response observed at low Q was highly anisotropic and exhibited a two-fold symmetry. This can only be the result of an oriented set of large plates. The scattering anisotropy can be analyzed by averaging the data over pie-shaped regions of the detector. As an example, the magnitude of the anisotropy and changing Q dependence of the $\alpha' \rightarrow \alpha$ scattering response (Fig. 3 data) is illustrated in Fig. 4, a comparison of the 50° and -40° sector averages. The 50° sector exhibits strong Porod scattering over most of the measured range (only the intermediate Q configuration data are shown), while the -40° sector data is pure Q^{-2}. The complete sector averages for the two radial-averaged data sets in Fig. 3 are shown in Fig. 5 as Porod amplitude (given as $4\pi\Delta\rho^2 S/V$) versus detector azimuthal angle. Three important facts can be stated regarding a comparison of the $\alpha \rightarrow \alpha'$ to the $\alpha' \rightarrow \alpha$ sector-average data: i) the peak Porod amplitude is a factor of 250 times larger for the dissolution sample, ii) the Porod scattering is highly anisotropic in both cases and is, therefore, the result of scattering from aligned, anisometric particles, and iii) the orientation of the particles rela-

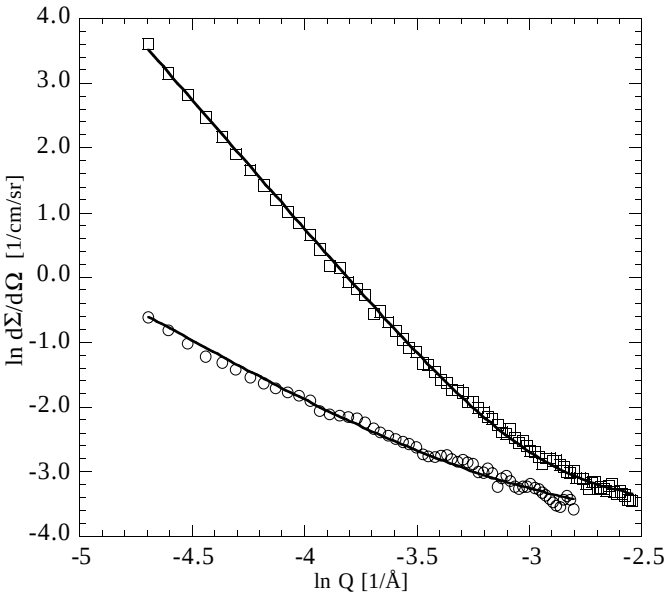

Figure 4
Two sector-average data sets for the 0.43 [D]/[Pd] concentration desorption measurement in ln-ln format. The 50° sector average (open boxes) follows a pure Porod scattering law over most of the intermediate Q range and corresponds to the direction of strongest scattering. The -40° sector average (open circles) follows a pure Q^{-2} scattering law and is much weaker.

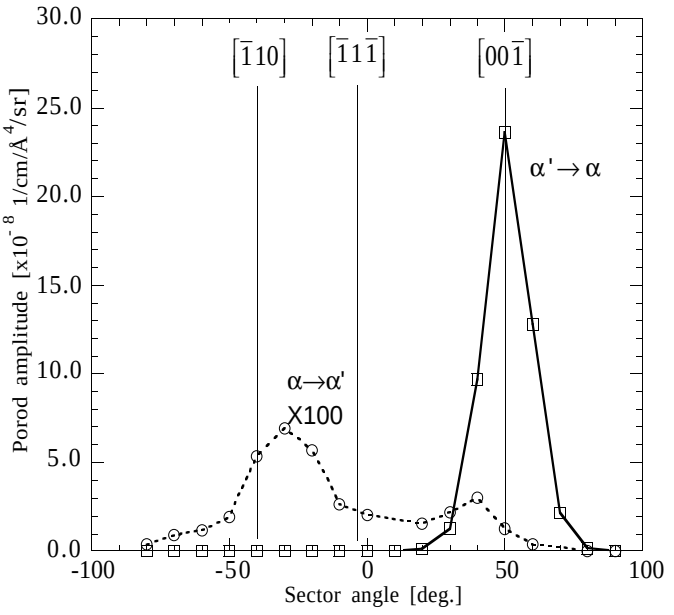

Figure 5
Variation of Porod scattering amplitude versus detector azimuthal or sector angle for the 0.060 [D]/[Pd] (dotted line) and 0.43 [D]/[Pd] (solid line) concentration data. Sector averaged data was determined by averaging over ± 5° angular intervals about the specified sector angle. Three high symmetry lattice directions contained in the measured Q plane are shown as vertical lines. The desorption or deuteride reversion data is highly anisotropic along the <100> direction, indicating plate-like particle formation on the {100} habit plane. The absorption data is also anisotropic, but along the <110> direction. The 0.060 [D]/[Pd] data have been multiplied by 100.

tive to the host lattice is different in each case.

We note here the incorrect assignment of the sample crystallographic orientation in a previous publication (Heuser *et al*., 1999), where the deuteride formation habit plane was mistakenly identified as $\{100\}_\alpha$. The correct sample orientation, leading to the $\{110\}_\alpha$, habit plane designation shown in Fig. 5, has been confirmed by x-ray diffraction measurements of {222} reciprocal lattice points in asymmetric reflection geometry (Heuser *et al*, 2000).

The observation of both the small and large plate-like particles is consistent with existing elasticity theory. Eshelby (1957) has shown that the total elastic energy is independent of the shape for coherent particle embedded in an elastically isotropic lattice. The equilibrium particle shape will then be determined by other effects such as interfacial energy, which could favor a spherical shape. However, both Pd and Pd hydride are anisotropic and have similar elastic constants (Hsu and Leisure, 1979). Lee *et al.* (1977) have calculated the elastic strain energy for a similar case (Ag precipitates in a Cu matrix) and demonstrate i) that an oblate ellipsoid of revolution is favored and ii) that the strain energy depends on the orientation relationship between precipitate and matrix and on the particle aspect ratio. The orientation dependence is most severe as the aspect ratio approaches zero (infinitely-flat ellipsoid) and favors the {100} habit plane. However, the differences in strain energy diminish as the particle geometry becomes less oblate (Lee *et al*., 1977). Although the Q^{-2} SANS response does not provide direct proof, it is reasonable to assume that the aspect ratio of coherent 20 to 30 Å plates is closer to 0.2 than to zero. Under these conditions, the strain energies calculated by Lee *et al*. (1977) for different habit planes (again for Ag precipitates in Cu) are within 20%. A similar effect in Pd would explain the lack of a preferred habit plane for the small, coherent plate formation implied by the isotropic Q^{-2} scattering response.

The large, oriented plates observed to form on the {100} habit plane during desorption are microns thick (because the Porod response occurs at lowest Q) and therefore must be semi-coherent or completely incoherent. Coherent shear stresses are eliminated during the loss of coherency and the precipitate is under a purely hydrostatic stress due to volume mismatch with respect to the host lattice. Elastic strain energy calculations have been performed for incoherent precipitates by Lee and Johnson (1978) and by Nabarro (1940). This work demonstrates that a flattened ellipsoid is favored for incoherent particles. Although the effect of orientation relationships for incoherent precipitates was not investigated by Lee and Johnson (1978) or by Nabarro (1940), the {100} habit plane observed during decomposition is consistent with a minimization of the elastic strain energy along the softest fcc lattice direction. On the other hand, the {110} habit plane observed during deuteride formation cannot be explained by these arguments. As explained previously (Heuser *et al*., 1999), large deuterium gas over-pressures (100 to 170 Torr above the 65 Torr plateau pressure) were required to promote deuteride precipitation during the room temperature absorption SANS measurements. We now believe the {110} habit plane represents a metastable precipitation configuration induced by the large over-pressure loading conditions and, possibly, the influence of the sample free surface. The observation of the {100} habit during desorption indicates a more equilibrium precipitation process, perhaps facilitated by heterogeneous nucleation at

dislocation defects created during the formation of the incoherent deuteride phase.

Acknowledgment is made to the donors of The Petroleum Research Fund, administered by the ACS, for support of this research. This research is also based upon activities supported by the National Science Foundation under Agreement No. DMR-9423101. The support of the National Institute of Standards and Technology, US Department of Commerce, in providing the facilities used in this experiment is gratefully acknowledged. The authors greatly appreciate the assistance of Dr. S. Kline (NIST).

References

Cahn, J.W. & Larché, F. (1984). *Acta Metall.* **32**, 1915-1923.
Eshelby, J.D. (1957). *Proc. R. Soc. A* **241**, 376-396.
Flanagan, T.B., Bowerman, B.S., & Biehl, G.E. (1980). *Scripta Metall.* **14**, 443-447.
Flanagan, T.B. & Clewley, J.D. (1982). *J. Less-Common Metals* **83**, 127-141.
Heuser, B.J., King, J.S. & Chen, W.C. (1999). *J. Alloys & Compounds* **292**, 134-147.
Heuser, B.J., King, J.S. & Chen, W.C. (2000). *J. Alloys & Compounds*, in press.
Hsu, D.K. & Leisure, R.G. (1979). *Phys. Rev. B* **20**, 1339-1344.
Jamieson, H.C., Weatherly, G.C.F.D. Manchester, F.D. (1976). *J. Less-Common Metals* **50**, 85-102.
Lee, J.K. & Johnson, W.C. (1978). *Acta Met.* **26**, 541-545.
Lee, J.K., Barnett, D.M., & Aaronson, H.I. (1977). *Met. Trans. A* **8A**, 963-970.
Lewis, F.A. (1967). *The Palladium/Hydrogen System*, pp. 23. London: Academic Press.
Lynch, J.F., Clewley, J.D., Curran, T., & Flanagan T.B. (1977). *J. Less-Common Metals* **55**, 153-163.
Nabarro, F.R. (1940). *Proc. R. Soc. (A)* **175**, 519-538.
Porod, G. (1982). *Small Angle X-ray Scattering* (Ed. O. Glatter and O. Kratky), pp. 17. London: Academic Press.
Porter, D.A. & Easterling, K.E. (1992). *Phase Transformations in Metals and Alloys, 2nd Ed.*, London: Chapman & Hall.
Roth, M. (1977). *J. Appl. Cryst.* **10**, 172-176
Schwarz, R.B. & Khachaturyan, A.G. (1995). *Phys. Rev. Lett.* **74**, 2523-2526.

 Received 17 May 1999 • Accepted 28 October 1999